Supporting Information

Ouyang *et al.* 10.1073/pnas.0807537105

SI Text

Methods

Cell Culture and Transfection. Cell culture reagents were obtained from GIBCO BRL. HeLa, MEF, and HEK 293 cells (from ATCC) were cultured in DMEM supplemented with 10% FBS, 2 mM L-glutamine, 100 unit/ml penicillin, 100 μg/ml streptomycin, and 1 mM sodium pyruvate in a humidified 95% air, 5% CO_2 incubator at 37°C before imaging.

The different DNA plasmids were transfected into cells by using Lipofectamine 2000 according to the manual protocol (Invitrogen).

Reagents and Plasmids. The Rac biosensor pRaichu-Rac1/RacCT is a gift from Dr. Michiyuki Matsuda at Kyoto University, Japan. The Ca^{2+} biosensor containing cpVenus (YC3.6) is from Dr. Atsushi Miyawaki at Brain Science Institute, RIKEN, Japan. Human MT1-MMP construct is a gift from Stephen J. Weiss at University of Michigan, Ann Arbor. The mCherry-Actin construct is from Dr. Ben N.G. Giepmans at University Medical Center Groningen, the Netherlands. Vav2 construct was purchased from Addgene, Inc. The plasmids of RacN17 and RacV12 were previously described by Li *et al.* (1).

Epithelial growth factor (EGF) purified from murine submaxillary gland, recombinant rat PDGF, Cytochalasin D and Nocodazole were purchased from Sigma-Aldrich. The recombinant VEGF was purchased from Upstate.

Micropatterning. Glass cover slips (Fisher Scientific, Pittsburgh, PA) were cleaned with a solution containing 98% H_2SO_4 and 30% H_2O_2 (volume ratio = 3:1) before the silanization in 2% dimethyl dichlorosilane (Sigma-Aldrich) in dichlorobenzene for 10 sec. The treated slips were then rinsed with acetone, ethanol and water, blown dry, and oxidized by UV-generated ozone (UVO Cleaner; Jelight, Irvine, CA) for 1 min (2). The PDMS microchannel mold was created by soft lithography as described previously (3). In brief, negative photo-resist Epon SU8 2015 was coated on a silicon wafer, which was then exposed to UV light through a transparency mask with parallel lines and spacing (30 and 10 μm in width, respectively) before being developed. PDMS prepared by mixing two liquid components (Sylgard 184 Kit, Dow Corning) was poured onto the developed wafer and cured. After solidification, the PDMS mold with microgrooves was peeled off and sealed on treated cover slips to create microfluidic channels. Fibronectin (Fn) solution (40 μg/ml) was then perfused through the channel driven by pressure gradient to coat the cover slips with defined parallel lines (10 μm in width with 30 μm spacing). The cover slips were then backfilled with pluronic acid (F127) (BASF Corporation, 0.5% in PBS) to prevent the cell adhesion on the remaining areas.

After transfected with different constructs for 36–48 h, cells were detached by 4 mM EDTA (pH 7.4) in PBS and seeded on Fn-coated patterns for 3–6 h before PDGF stimulation.

Protein Expression and *in Vitro* Assay. Chimeric proteins were expressed with N-terminal 6x *His* tag in *Escherichia coli* and purified by nickel chelation chromatography as described (4). Fluorescence emission spectra of the purified biosensors with a final concentration of 1 μM were measured in a 96-well plate with an excitation wavelength of 430 nm by a fluorescence plate reader (TECAN, Sapphire II). For the detection of Src FRET biosensors, emission ratios of donor/acceptor (478 nm/526 nm) were measured at 37°C before and after the addition of 1 mM ATP in a Src kinase buffer (4) containing 01.1 μg/ml active Src kinase (Upstate). For Rac biosensor assay, the negative (N17) and active (V12) mutants of biosensor DNAs were transfected into HEK293 cells for 48 h. Then cells were tryposinized and suspended into PBS and the donor/acceptor emission ratios (478 nm/526 nm) were measured immediately in a 96-well plate by the fluorescence plate reader. For Ca^{2+} biosensor assay, acceptor/donor emission ratios (526 nm/478 nm) were measured in calcium-saturated vs. calcium-free PBS solutions by supplementing with 1 mM $CaCl_2$ or 1 mM EGTA, respectively. For MT1-MMP biosensor assay, donor/acceptor emission ratios (478 nm/526 nm) were measured at 37°C before and after adding the recombinant catalytic domain of human MT1-MMP (CAT) (2 μg/ml, Calbiochem) into the MT1-MMP proteolysis assay buffer (50 mM Hepes, 10 mM $CaCl_2$, 0.5 mM $MgCl_2$, 50 μM $ZnCl_2$, and 0.01% Brij-35, pH 6.8) (5).

1. Li S, *et al.* (1999) Distinct roles for the small GTPases Cdc42 and Rho in endothelial responses to shear stress. *J Clin Invest* 103:1141–1150.
2. Tan JL, Liu W, Nelson CM, Raghavan S, Chen CS (2004) Simple approach to micropattern cells on common culture substrates by tuning substrate wettability. *Tissue Eng* 10:865–872.
3. Whitesides GM, Ostuni E, Takayama S, Jiang X, Ingber DE (2001) Soft lithography in biology and biochemistry. *Annu Rev Biomed Eng* 3:335–373.
4. Wang Y, Botvinick EL, Zhao Y, Berns MW, Usami S, Tsien RY, Chien S (2005) Visualizing the mechanical activation of Src. *Nature* 434:1040–1045.
5. Rozanov DV, Deryugina EI, Monosov EZ, Marchenko ND, Strongin AY (2004) Aberrant, persistent inclusion into lipid rafts limits the tumorigenic function of membrane type-1 matrix metalloproteinase in malignant cells. *Exp Cell Res* 293:81–95.

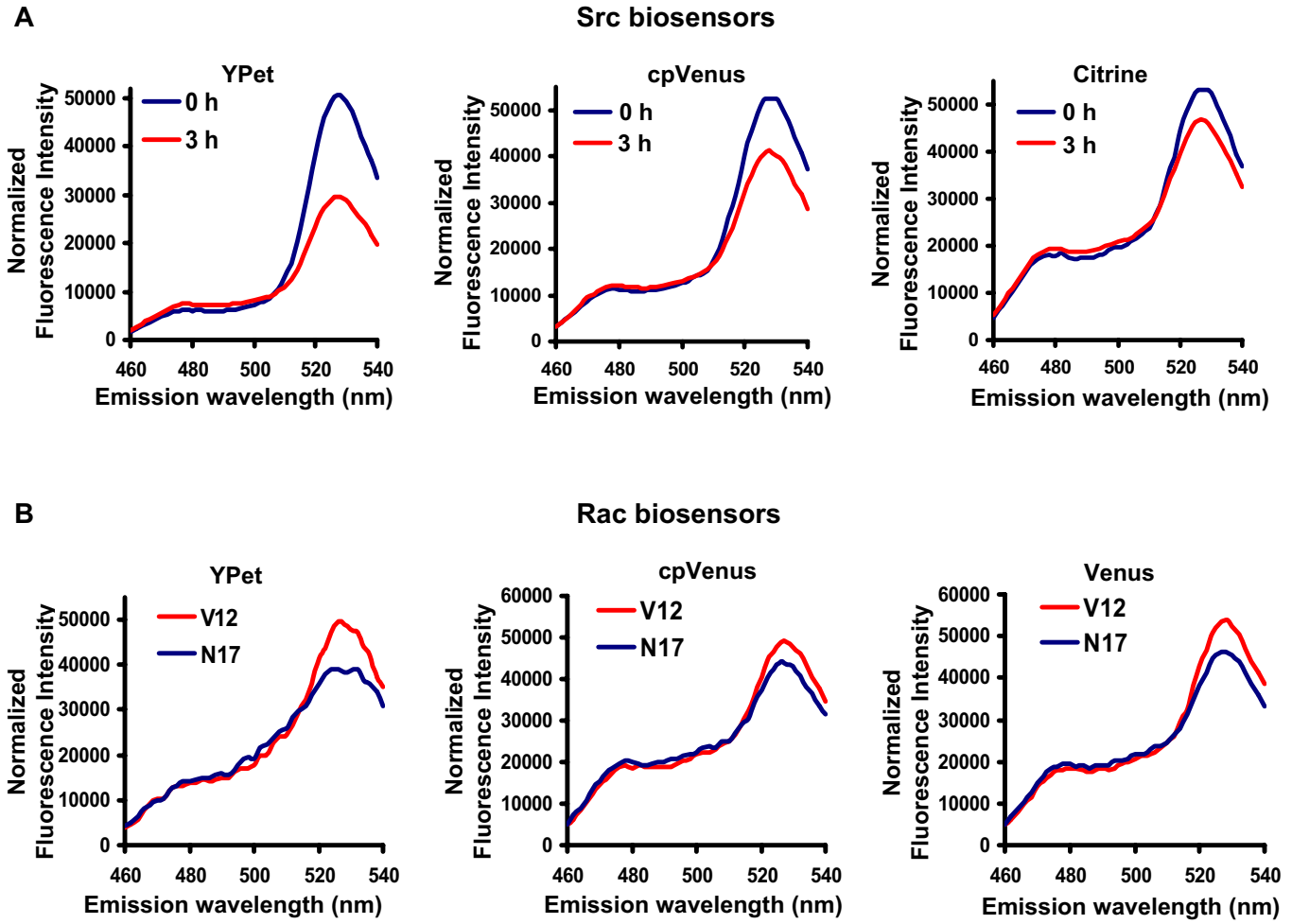

Fig. S1. (*A*) Emission spectra of purified Src biosensors (with YPet, cpVenus, or Citrine as the FRET acceptor) before (blue) and after (red) incubation with Src kinase for 3 h. (*B*) Emission spectra of Rac biosensors (with YPet, cpVenus, or Venus as the FRET acceptor) with negative (N17, blue) and active (V12, red) mutations.

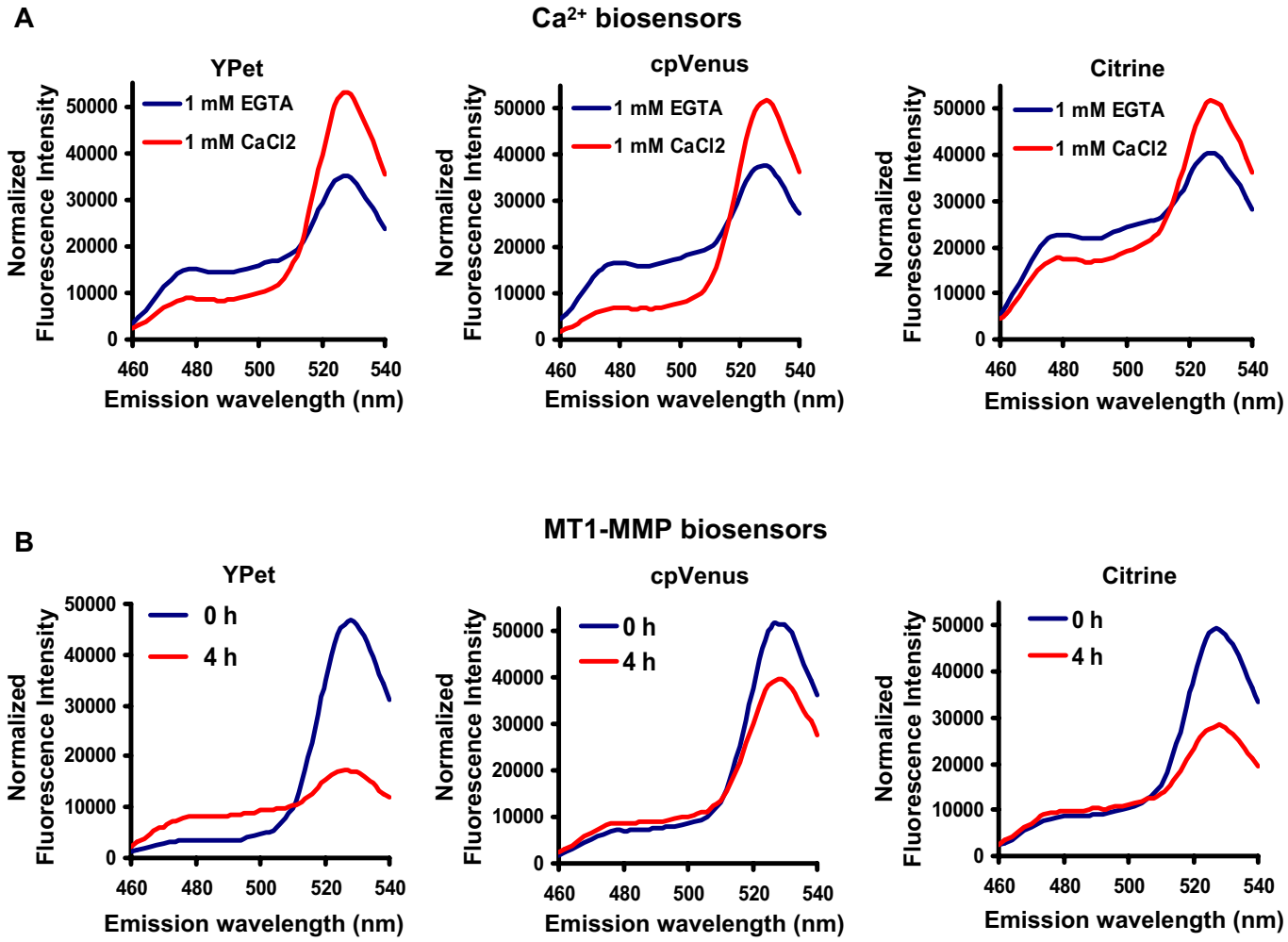

Fig. S2. (*A*) Emission spectra of purified Ca^{2+} biosensors (with YPet, cpVenus, or Citrine as the FRET acceptor) incubated with 1 mM EGTA (Ca^{2+}-free, blue) or 1 mM $CaCl_2$ (saturated Ca^{2+}, red). (*B*) Emission spectra of purified MT1-MMP biosensors (with YPet, cpVenus, or Citrine as the FRET acceptor) before (blue) and after (red) incubation with the catalytic domain of MT1-MMP for 4 h.

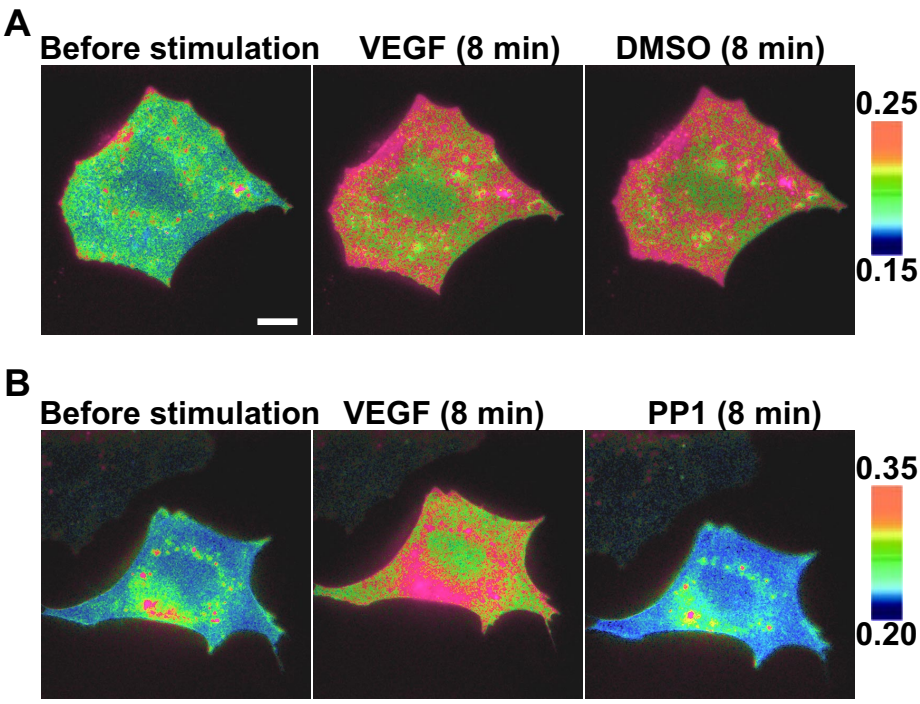

Fig. S3. Emission ratio images of the ECFP/YPet-based KRas-Src biosensor in BAECs before and after the treatment with 50 ng/ml VEGF, followed by the incubation with (*B*) 10 μM PP1 or (*A*) its control solvent DMSO for the time periods as indicated. (Scale bar: 30 μm.)

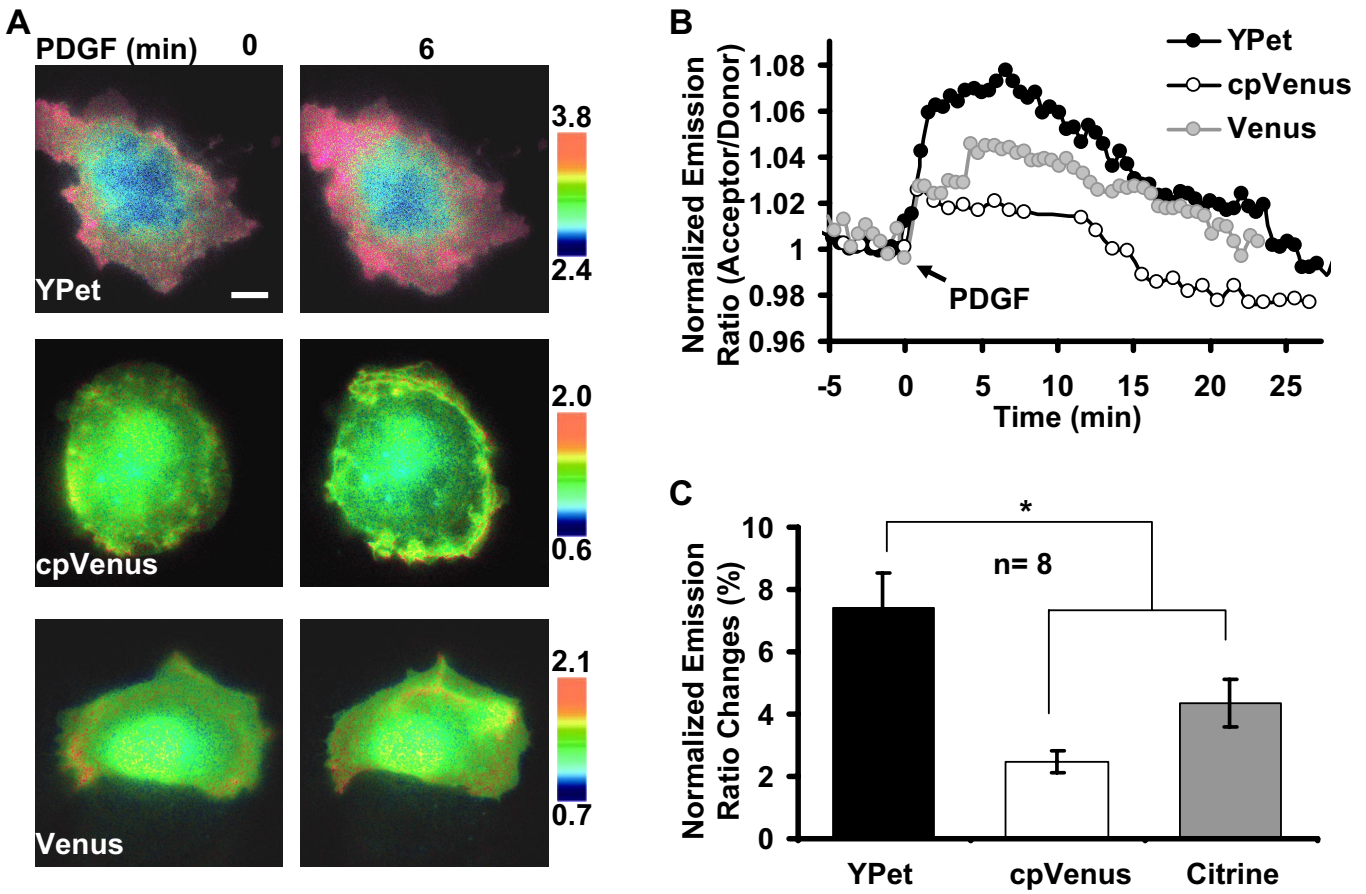

Fig. S4. PDGF-induced response of Rac biosensors in MEF cells seeded on Fibronectin-coated dishes. (*A*) Emission ratio images of Rac biosensors (with YPet, cpVenus or Venus as the FRET acceptor) before and after treatment with 50 ng/ml PDGF in MEF cells. (*B*) Emission ratio time courses of the Rac biosensors in response to PDGF stimulation in *A*. (*C*) Bar graphs represent the emission ratio changes of Rac biosensors from multiple cells (mean ± SEM.). ''n'' represents the cell number in each group. ''*'' indicates the significant difference between different groups. (Scale bar: 30 μm.)

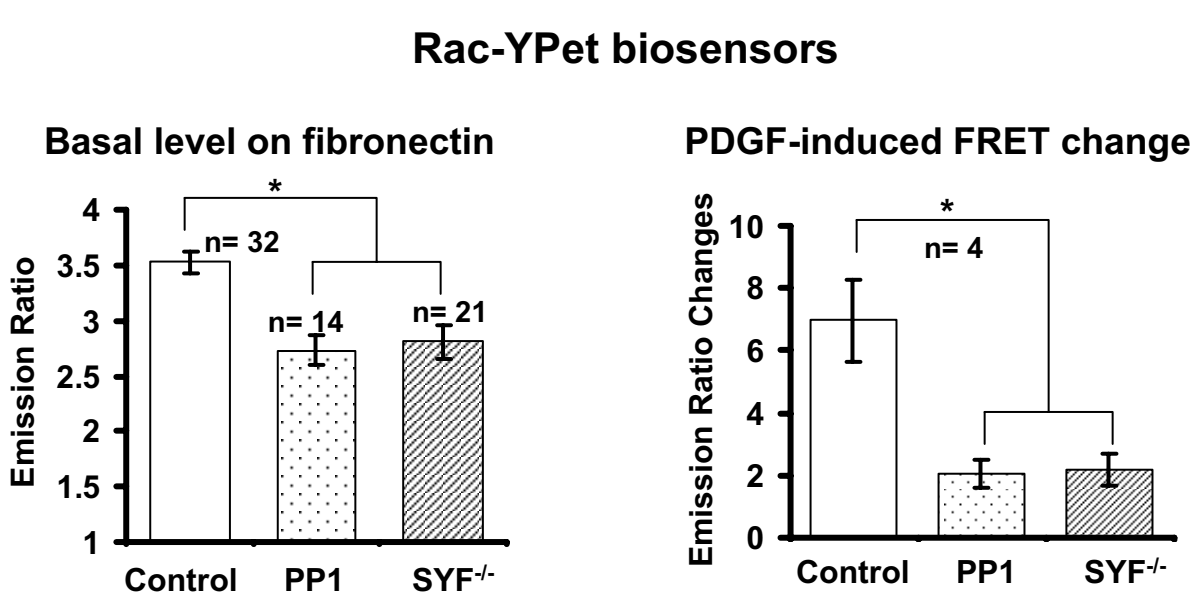

Fig. S5. Src mediates the Rac activation. All of the cells were cultured on fibronectin. (*A*) Bar graphs represent the basal levels of emission ratio (mean ± SEM.) of the ECFP/YPet Rac biosensor in control or PP1 pretreated MEF cells, or in SYF-/- cells. (*B*) Bar graphs represent the emission ratio changes (mean ± SEM) of the ECFP/YPet Rac biosensor in response to 50 ng/ml PDGF in control or PP1 pretreated MEF cells, or in SYF-/- cells. '*' indicates a significant difference between groups.

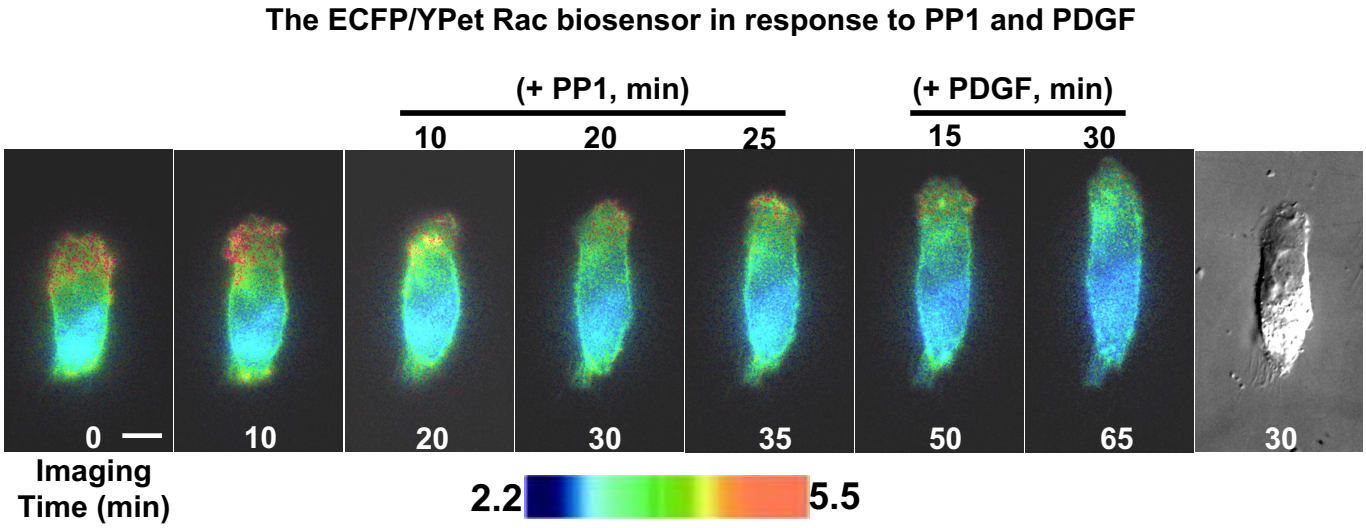

Fig. S6. Emission ratio imaging of the ECFP/YPet-based Rac biosensor in MEF cells cultured on fibronectin-coated stripes before and after the treatment with 10 μM PP1, followed by the images addition of 50 ng/ml PDGF as indicated. (Scale bar: 30 μm.)

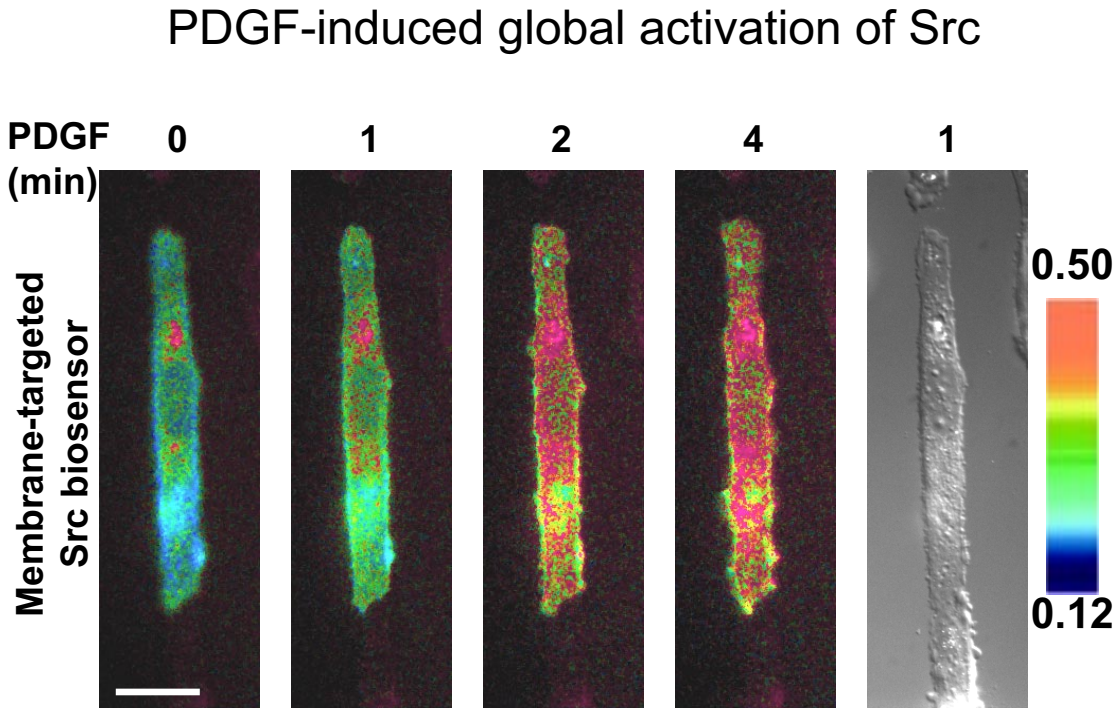

Fig. S7. PDGF-induced global activation of Src in MEF cells. Emission ratio images of the ECFP/YPet-based and membrane-targeted Src biosensor in a MEF cell cultured on Fibronectin-coated stripes before and after 50 ng/ml PDGF stimulation. (Scale bar: 30 μm.)

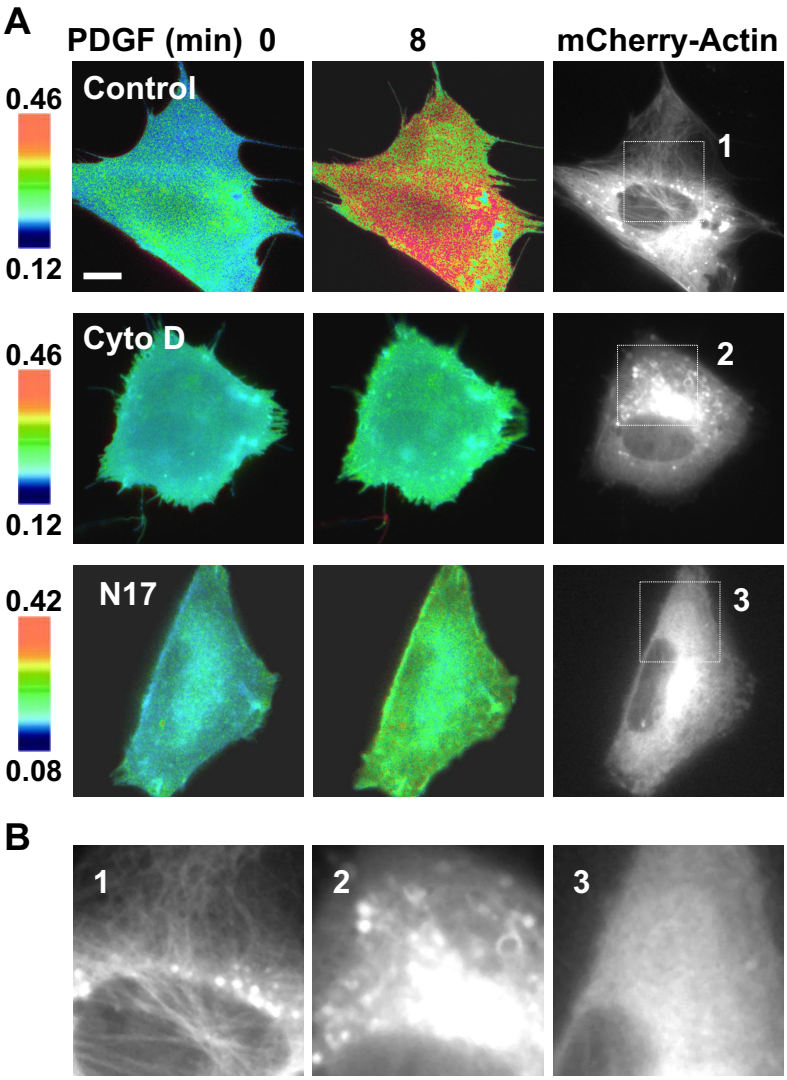

Fig. S8. (*A*) The emission ratio images of the membrane-targeted Src biosensor (*Left*) and mCherry-actin images (*Right*) in MEF cells: control, pretreated by 1 μM CytoD for 1 h or cotransfected with RacN17, before and after they were subjected to PDGF stimulation. (*B*) Enlarged images of selected regions in *A* showing the actin filaments represented by the mCherry-actin fluorescence. (Scale bar: 30 μm.)

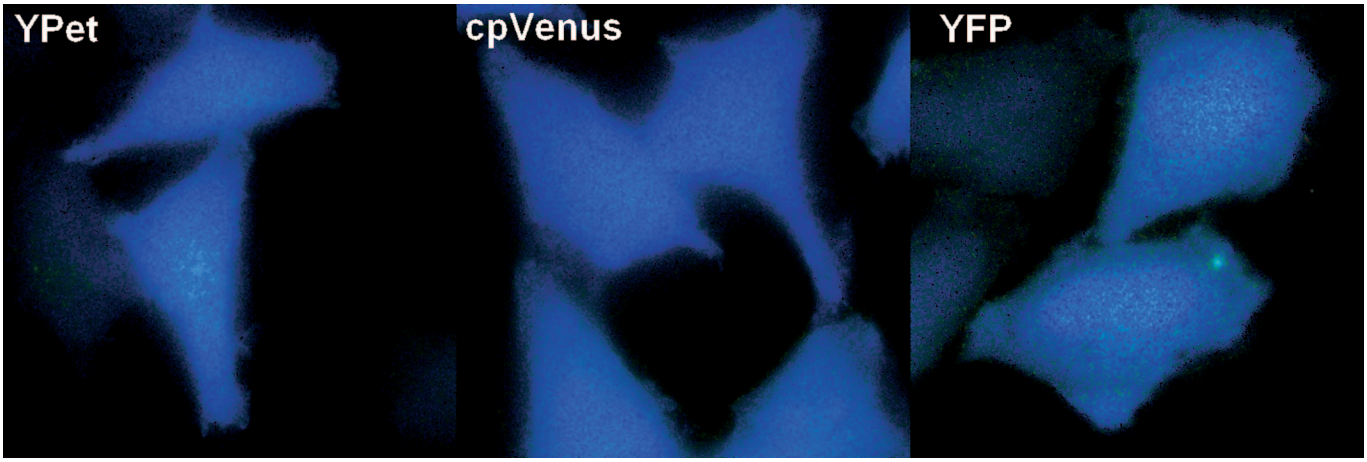

Movie S1. PVD-induced FRET response in HeLa cells expressing the Src biosensors (with YPet, cpVenus, or Citrine as the FRET acceptor, as indicated).

Movie S1 (AVI)

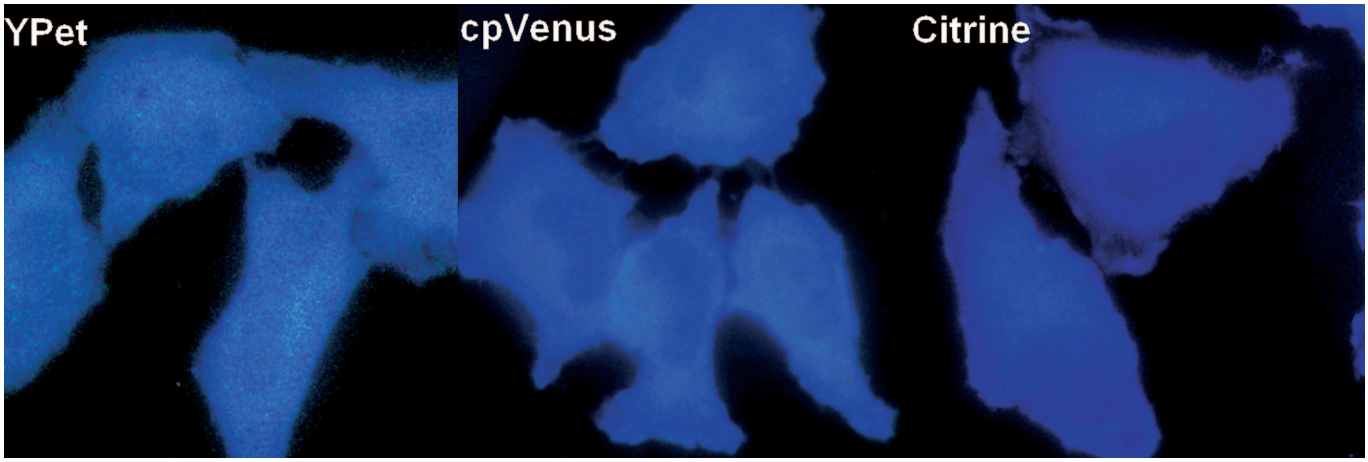

Movie S2. ATP-induced oscillatory FRET response in HeLa cells expressing the Ca^{2+} biosensors (with YPet, cpVenus, or Venus as the FRET acceptor, as indicated).

Movie S2 (AVI)

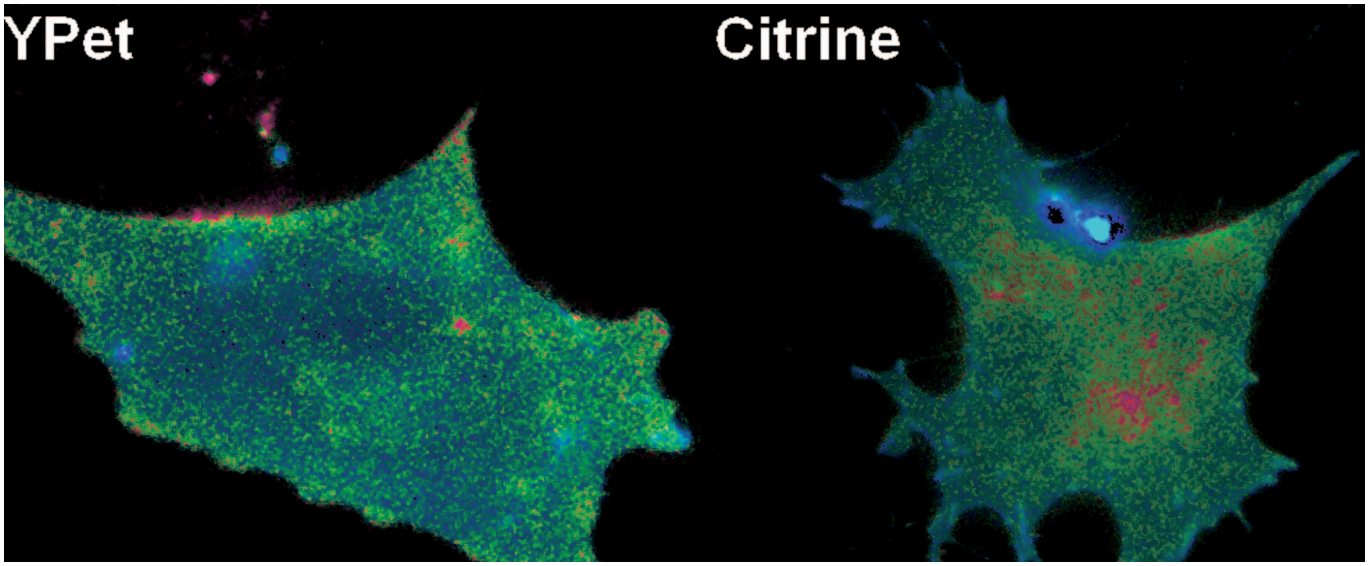

Movie S3. VEGF-induced FRET response in BAECs expressing the membrane-targeted Src biosensors (with YPet or Citrine as the FRET acceptor, as indicated).

Movie S3 (AVI)

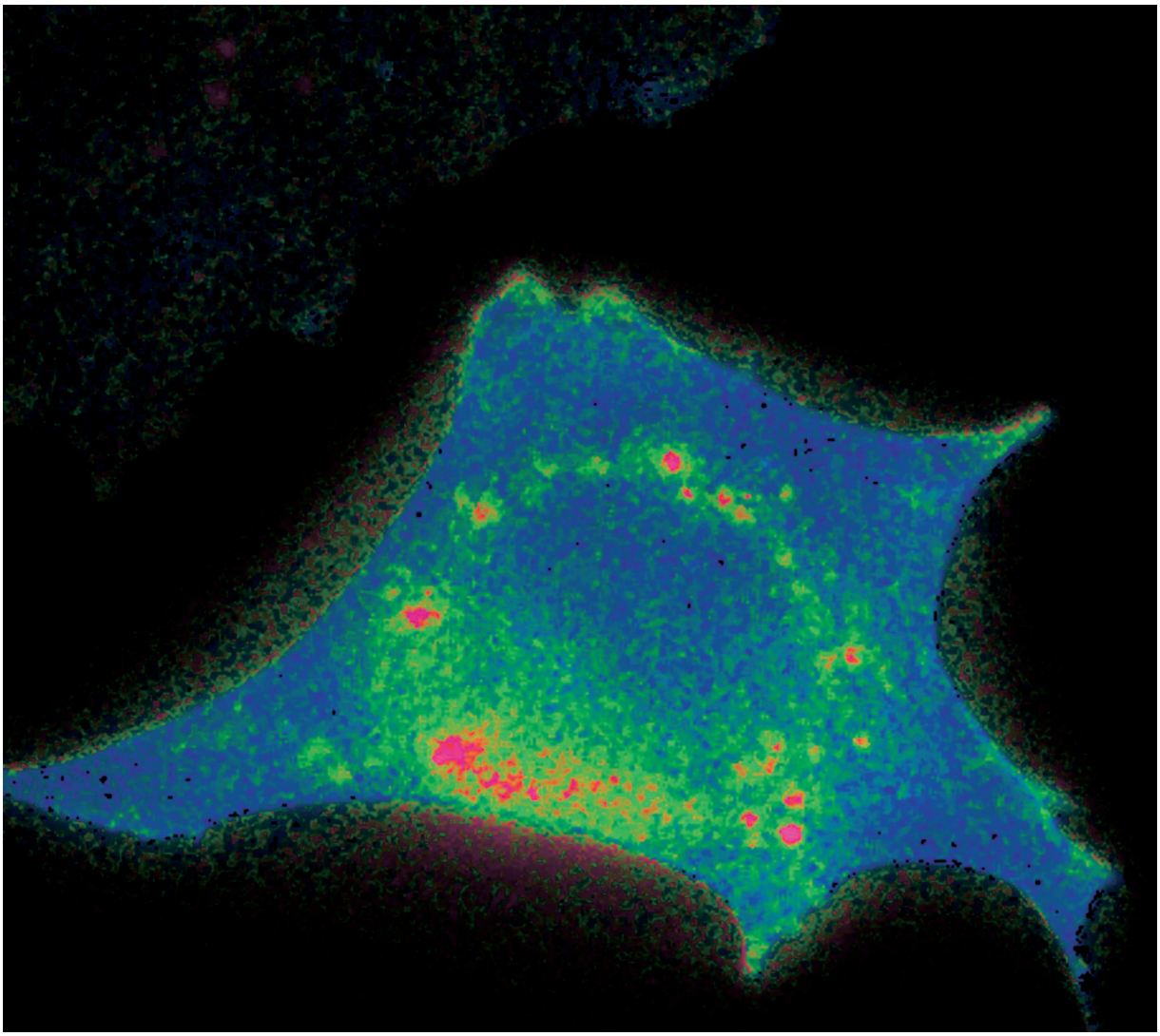

Movie S4. PP1 reversed the FRET response of the ECFP/YPet-based Src biosensor in BAECs induced by VEGF.

Movie S4 (AVI)

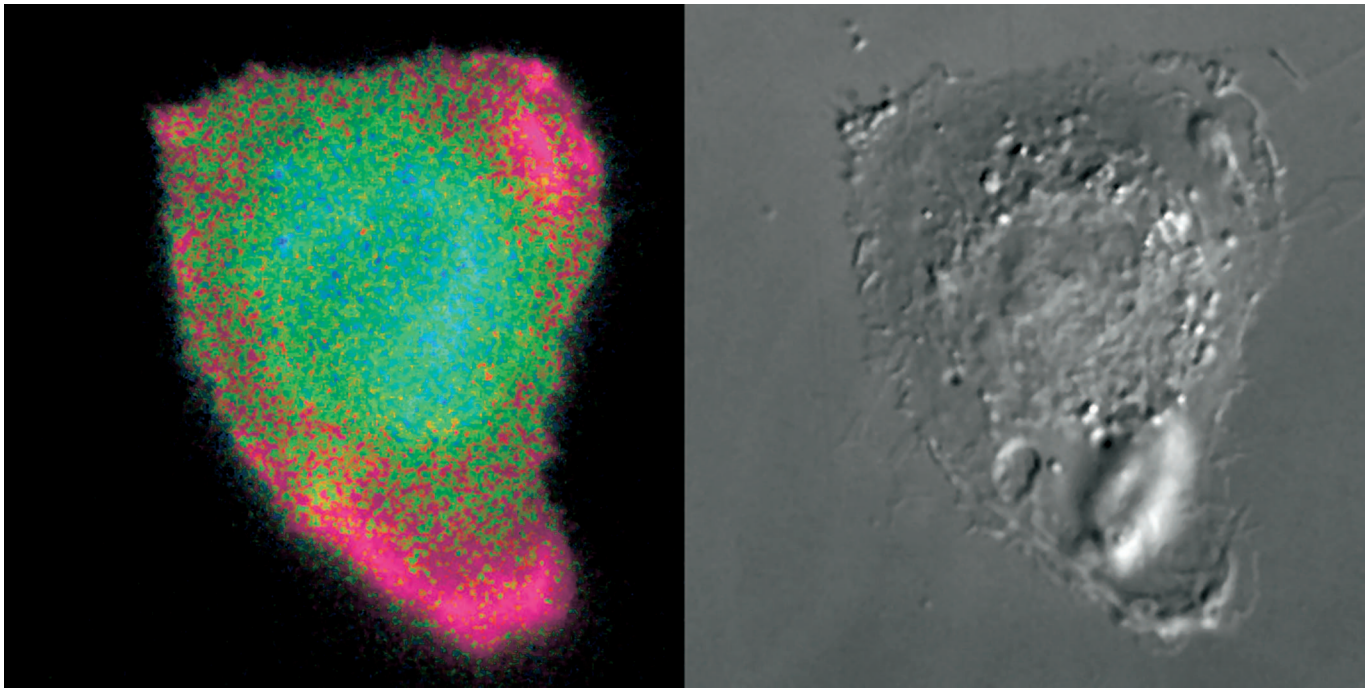

Movie S5. PDGF-induced Rac activation at membrane rafts visualized by the ECFP/YPet-based Rac biosensor. (*Left*) Acceptor/donor Emission Ratio Image. (*Right*) DIC image.

Movie S5 (AVI)

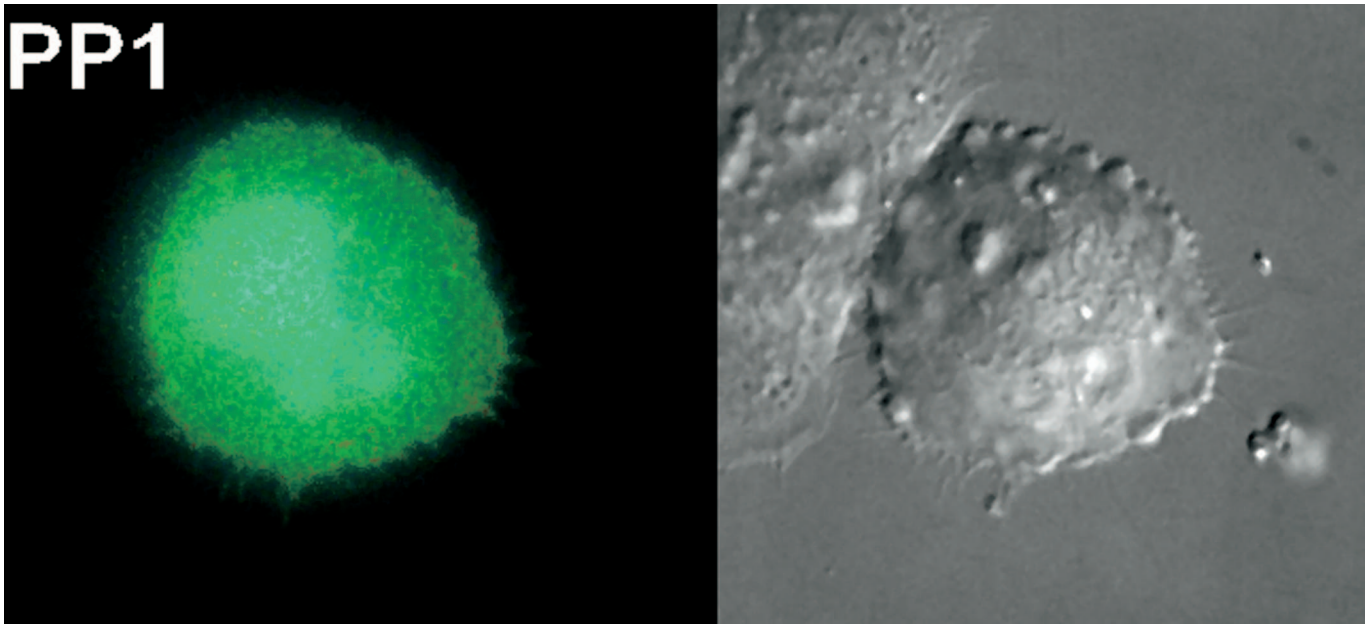

Movie S6. PP1 inhibited the PDGF-induced Rac activation at membrane rafts visualized by the ECFP/YPet-based Rac biosensor. (*Left*) Acceptor/donor Emission Ratio Image. (*Right*) DIC image.

Movie S6 (AVI)

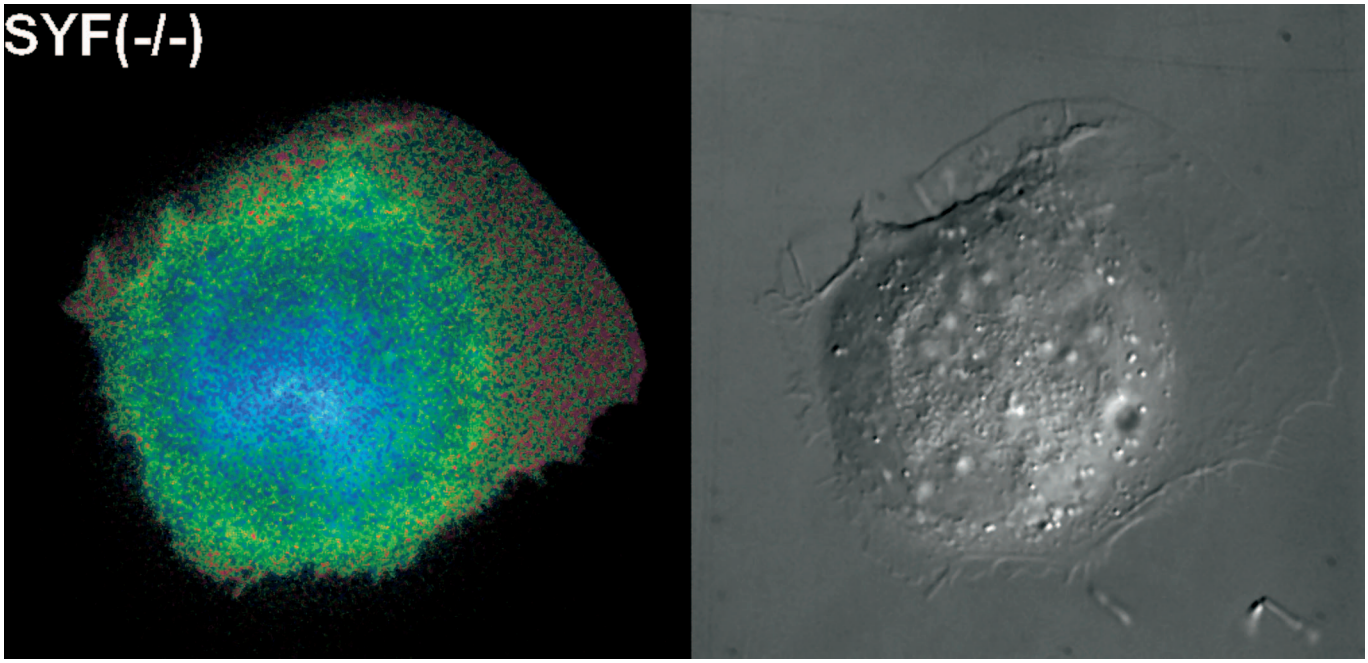

Movie S7. The PDGF-induced Rac activation is significantly inhibited in SYF-/- cells. (*Left*) Acceptor/donor Emission Ratio Image. (*Right*) DIC image.

Movie S7 (AVI)

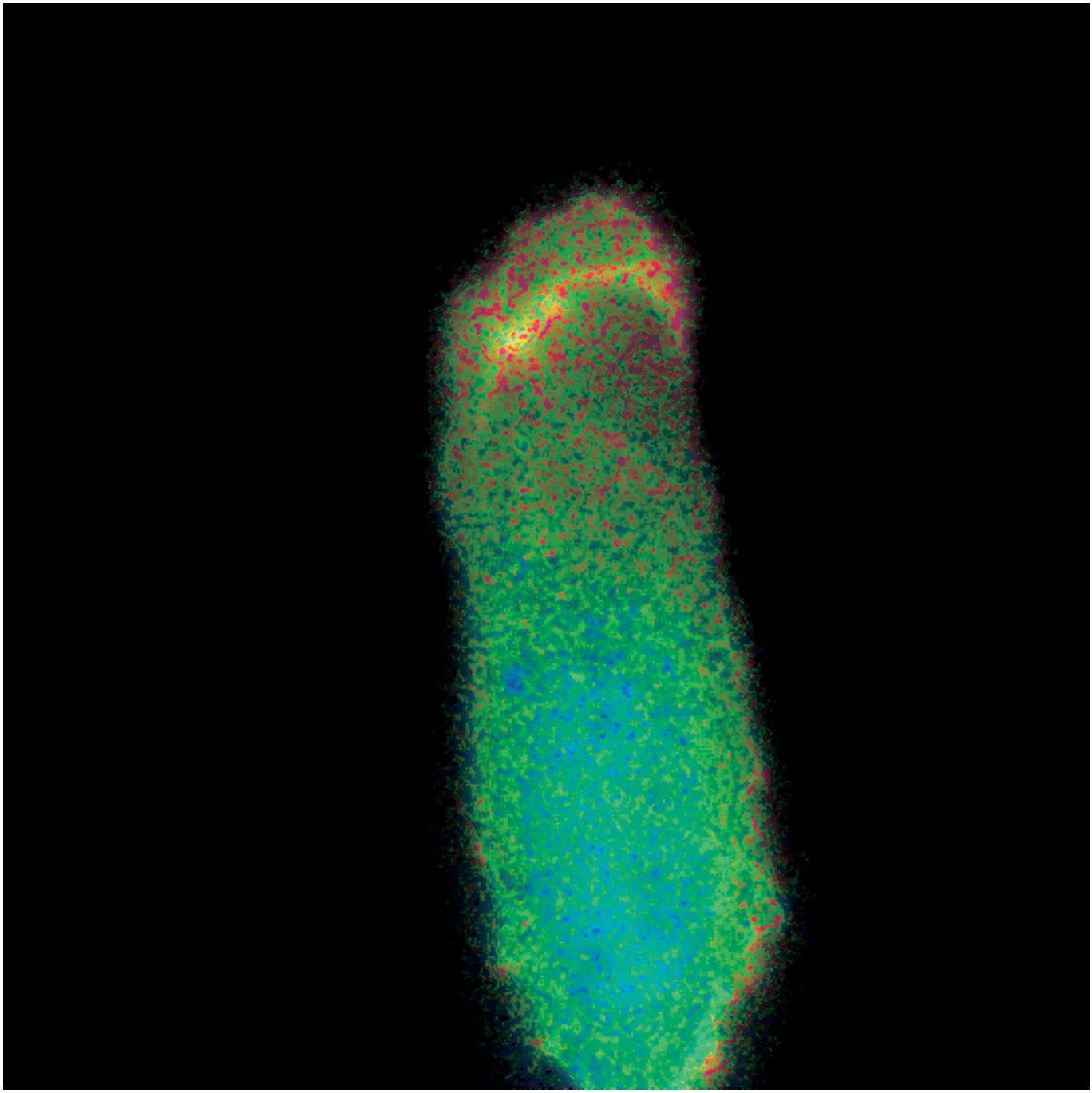

Movie S8. PDGF induced a significant Rac polarization in MEF cells migrating on Fn-coated stripes (10 μm in width).

Movie S8 (AVI)

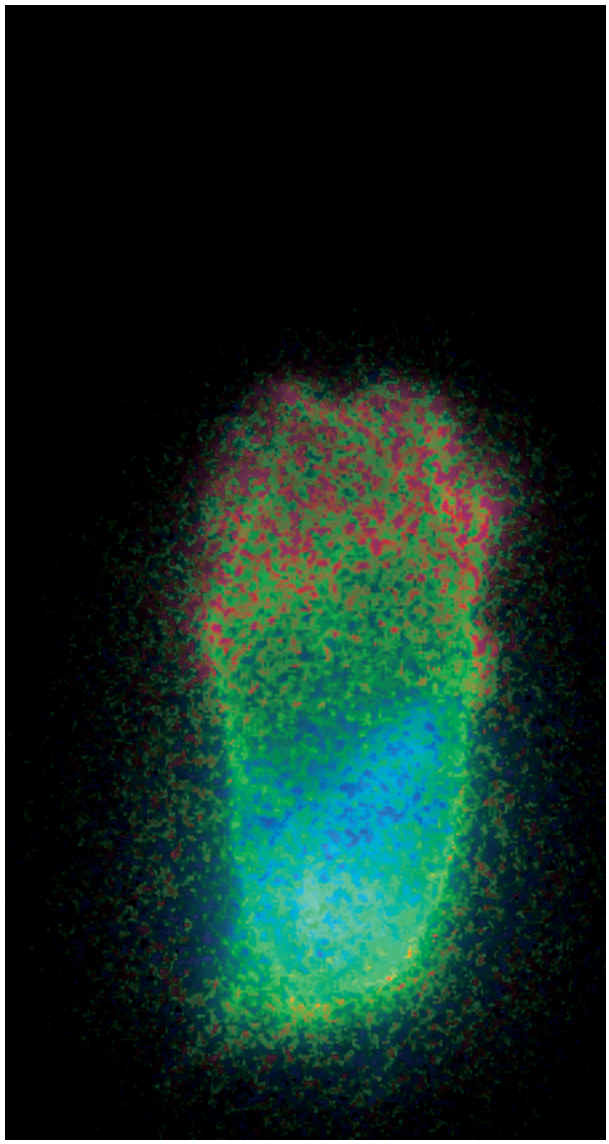

Movie S9. PP1 inhibited the polarized Rac activity in MEF cells migrating on Fn-coated stripes (10 μm in width) and their response to PDGF stimulation.

Movie S9 (AVI)

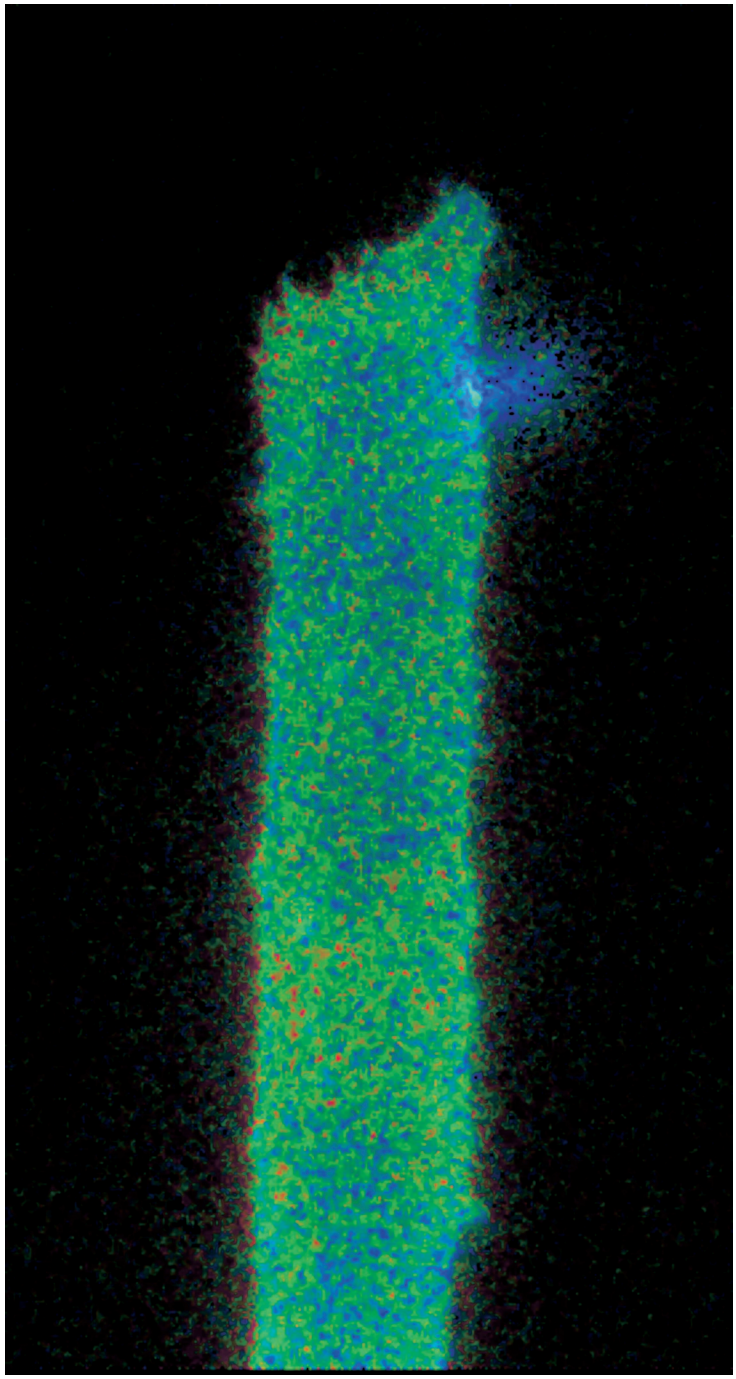

Movie S10. PDGF induced a global Src activation in MEF cells migrating on Fn-coated stripes (10 μm in width).

Movie S10 (AVI)

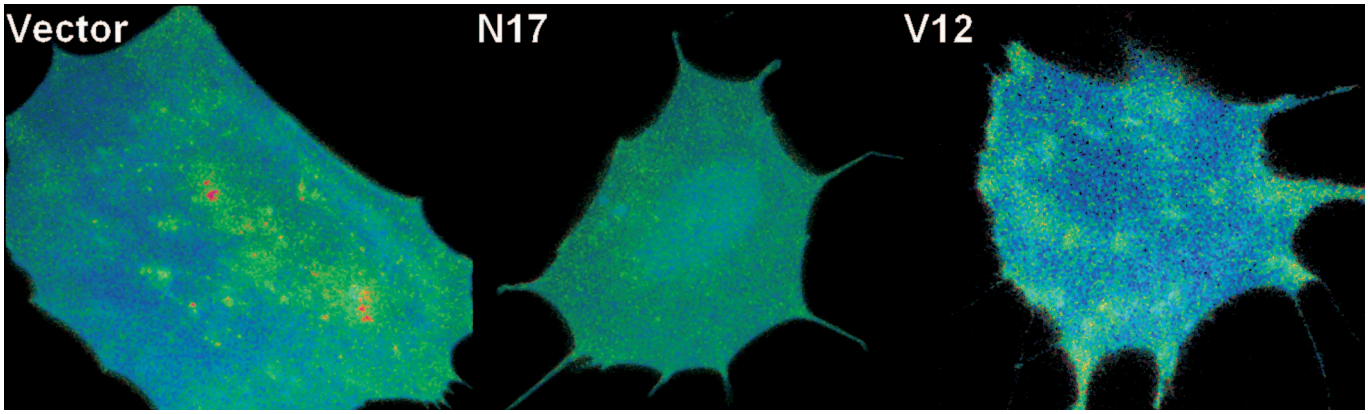

Movie S11. RacN17 inhibited while RacV12 enhanced the PDGF-induced Src activation.

Movie S11 (AVI)

Table S1. The sensitivities of biosensors with different FRET acceptors

	Dynamic range of purified biosensors, %			Dynamic range of biosensors in live cells, %		
Acceptors biosensors	Citrine or Venus	cpVenus	YPet	Citrine or Venus	cpVenus	YPet
Src (donor/acceptor)	25	40	120	32	77	176
Rac (acceptor/donor)	28	26	46	15	5	70
Ca^{2+} (acceptor/donor)	65	350	135	41	242	253
MT1-MMP (donor/acceptor)	100	90	570	13	12	50

Sensitivities of biosensors with different FRET acceptors *in vitro* and in mammalian cells.

Table S2. The settings of filters for fluorescence imaging

	Excitation filter, nm	Dichroic mirror (l,. . . after nm)	Emission filter, nm
CFP	420/20	450	475/40
YFP(FRET)			535/25
mCherry	560/40	595	653/95

Parameter settings of filters for fluorescence imaging.